Published in final edited form as:
J Mater Chem B. 2015 December 14; 3(46): 9067–9078. doi:10.1039/c5tb01645b.

Biofabrication of reinforced 3D-scaffolds using two-component hydrogels†

Kristel W. M. Boere[a], **Maarten M. Blokzijl**[a,b], **Jetze Visser**[b], **J. Elder A. Linssen**[b], **Jos Malda**[b,c], **Wim E. Hennink**[a], **Tina Vermonden**[‡,*,a]

[a]Department of Pharmaceutics, Utrecht Institute for Pharmaceutical Sciences (UIPS), Faculty of Science, Utrecht University, P. O. Box 80082, 3508 TB Utrecht, The Netherlands [b]Department of Orthopaedics, University Medical Center Utrecht, P.O. Box 85500, 3508 GA Utrecht, The Netherlands [c]Department of Equine Sciences, Faculty of Veterinary Medicine, Utrecht University, P.O. Box 80163, 3508 TD Utrecht, The Netherlands

Abstract

Progress in biofabrication technologies is mainly hampered by the limited number of suitable hydrogels that can act as bioinks. Here, we present a new bioink for 3D-printing, capable of forming large, highly defined constructs. Hydrogel formulations consisted of a thermoresponsive polymer mixed with a poly(ethylene glycol) (PEG) or a hyaluronic acid (HA) cross-linker with a total polymer concentration of 11.3 and 9.1 wt% respectively. These polymer solutions were partially cross-linked before plotting by a chemoselective reaction called oxo-ester mediated native chemical ligation, yielding printable formulations. Deposition on a heated plate of 37 °C resulted in the stabilization of the construct due to the thermosensitive nature of the hydrogel. Subsequently, further chemical cross-linking of the hydrogel precursors proceeded after extrusion to form mechanically stable hydrogels that exhibited a storage modulus of 9 kPa after 3 hours. Flow and elastic properties of the polymer solutions and hydrogels were analyzed under similar conditions to those used during the 3D-printing process. These experiments showed the ability to extrude the hydrogels, as well as their rapid recovery after applied shear forces. Hydrogels were printed in grid-like structures, hollow cones and a model representing a femoral condyle, with a porosity of 48 ± 2%. Furthermore, an N-hydroxysuccinimide functionalized thermoplastic poly-e-caprolactone (PCL) derivative was successfully synthesized and 3D-printed. We demonstrated that covalent grafting of the developed hydrogel to the thermoplastic reinforced network resulted in improved mechanical properties and yielded high construct integrity. Reinforced constructs also containing hyaluronic acid showed high cell viability of chondrocytes, underlining their potential for further use in regenerative medicine applications.

* T.Vermonden@uu.nl; Tel: (+31)620291631.
‡Current address: Department of Pharmaceutics, Utrecht Institute for Pharmaceutical Sciences, Utrecht University, Universiteitsweg 99, 3584 CG Utrecht, The Netherlands.

Europe PMC Funders Author Manuscripts

1 Introduction

Additive manufacturing is an emerging technique for the fabrication of complex three-dimensional (3D) constructs.[1–3] The manufacturing of constructs containing biological components is termed biofabrication and currently often used in the field of regenerative medicine. Inks for biofabrication are typically based on hydrogels, in which cells or bioactive factors can be encapsulated.[1,4–6] Complex geometries having a porous network can be created based on a computer-designed model, facilitating high diffusion of nutrients and metabolites required for tissue regeneration. Furthermore, a layer-controlled arrangement of different cell-types and biomolecules can be achieved by the incorporation of cells in the printing process. In this way, anatomical structures can be created such as those replicating blood vessel networks[7] or those mimicking the zonal architecture of cartilage.[8] Whilst hydrogels have been widely investigated for biomedical applications,[9–11] tuning their properties towards a favorable bioprinting strategy remains a challenge.[1,12]

Many established biofabrication approaches rely on hydrogel formation by temperature-induced physical cross-linking often combined with subsequent chemical cross-linking.[13–15] A drawback of these techniques is that a high polymer concentration is required to stabilize the hydrogel structure for printing multiple layers with high shape fidelity.[14,16] A high polymer content can potentially limit the diffusion of nutrients and metabolites, and can consequently have a negative impact on cell migration and proliferation.[17] Additionally, to stabilize the network, small molecules or UV light are frequently used to induce subsequent covalent cross-linking. Besides the difficulties to control the shape fidelity of the constructs, the effect of these methods on the cytotoxicity of cells is under debate.[9,18]

As an alternative for photopolymerization, chemoselective reactions offer exciting opportunities for the formation of biomaterials.[19] Oxo-ester mediated native chemical ligation (OMNCL) has been proposed as a promising reaction because of its high efficiency, mild reaction conditions and high selectivity.[20] This ligation reaction involves conjugation between an activated ester and an N-terminal cysteine and has been previously demonstrated to be highly compatible with incorporated cells and bioactive molecules.[21] Recently, we reported thermosensitive OMNCL cross-linked hydrogels that showed tunable degradation rates and mechanical properties.[22] Importantly, solutions of relatively low polymer concentrations of 12 wt% were transferred into mechanically stable hydrogels as a result of the combined physical and chemical cross-linking mechanism.

However, to enable bioprinting of hydrogels with solutions of low polymer concentrations, while still obtaining mechanically strong constructs with high shape fidelity, new biofabrication approaches have to be investigated.[1] Partial pre-crosslinking of the hydrogel precursors is an attractive approach to facilitate a good shape fidelity of printed constructs using low polymer concentrations.[23–25] Rutz et al.[24] described partial pre-crosslinking of functionalized poly(ethylene glycol) (PEG) cross-linkers with natural polymers, thereby forming a variety of 3D-printed hydrogels with low polymer contents. These bioinks were deposited with a low flow, without collapse and resulting constructs maintained high shape fidelity. However, the obtained hydrogel networks were still relatively soft, which could

hamper their potential therapeutic applications under for example load-bearing conditions where the gels are exposed to mechanical forces.

Mechanically strong constructs containing hydrogels with low polymer concentrations can be fabricated using multimaterial constructs based on hydrogels that are reinforced with a thermoplastic polymer network.[26–28] Poly-e-caprolactone (PCL) is a widely used thermoplastic polymer in biofabrication, given its relatively low melt processability (at 60 °C) and mechanical properties.[29] As an alternative for PCL, our group reported the use of a hydroxyl-functionalized variation, poly(hydroxymethylglycolide-co-e-caprolactone), abbreviated as pHMGCL.[30,31] Compared to PCL, pHMGCL showed increased degradation rates, improved cell adhesion and was shown to be 3D-printed with good shape fidelity.[32] Importantly, methacrylate groups can be introduced to allow covalent grafting of a hydrogel and thermoplastic after photopolymerization.[33] A synergistic effect on the mechanical properties of these hydrogel–thermoplastic constructs was found as a result of covalent grafting at the interface between the hydrogel and thermoplastic, which resulted in a remarkable stabilization and increased mechanical resistance against shear forces.[33]

In this study, the two novel approaches of partial pre-crosslinking and thermoplastic grafting were combined for the fabrication of a mechanically strong 3D-printed construct that was cross-linked by oxo-ester mediated native chemical ligation. Thermoresponsive hydrogels were used to obtain additional network stabilization as a result of physical cross-linking immediately after deposition on a heated plate. Furthermore, these hydrogels were covalently grafted to a strong thermoplastic scaffold for the formation of even more mechanically robust constructs. Covalent cross-linking by OMNCL within the hydrogel as well as between the hydrogel and thermoplastic material was assessed to obtain a mechanically strong and fully integrated construct.

2 Materials and methods

2.1 Materials

All chemicals were purchased from Sigma-Aldrich and used as received, unless stated otherwise. Hyaluronic acid (HA, 33 kDa) was obtained from Lifecore (Chaska, Mn, USA). Poly(hydroxy-methylglycolide-co-ε-caprolactone) (pHMGCL, 8% HMG) was synthesized according to literature procedures.[30] N-(2-Hydroxy-propyl)methacrylamide-Boc-S-acetamidomethyl-L-cysteine (Boc-Cys(Acm)-HPMA) was synthesized following a previously published procedure.[34] N-(3-Dimethylaminopropyl)-N’-ethyl-carbodiimide hydrochloride (EDCI) was purchased from Bachem (Bubendorf, Switzerland). PEG 20,000 8-arm with a tripentaerythritol core was obtained from JenKem Technology USA (Plano, Tx, USA). Ethylthioglycolate succinic acid (ET-SA) was synthesized according to a published procedure.[35] A PEG 10 000-(4,4’-azobis(4-cyanopentanoic acid)) (ABCPA) macro-initiator was synthesized following established procedures.[36] Tris(2-carboxyethyl)phosphine hydrochloride (TCEP) was obtained from Carl Roth (Karlsruhe, Germany) and 4-(dimethyl-amino)pyridinium-4-toluene-sulfonate (DPTS) was synthesized following published procedures.[37] Poly(ethylene glycol) standards for GPC analysis were obtained from PSS Polymer Standards Service GmbH (Mainz, Germany). Red food coloring agent Ponceau 4R, E number 124 was obtained from Queen Fine foods Pty. Ltd (Alderley

Q., Australia). Phosphate buffered saline (PBS) pH 7.4 (8.2 g L^{-1} NaCl, 3.1 g L^{-1} $Na_2HPO_4{\cdot}12H_2O$, 0.3 g L^{-1} $NaH_2PO_4{\cdot}2H_2O$) was purchased from B. Braun (Melsungen, Germany).

2.2 Synthesis of a PNC triblock copolymer

A PEG–NIPAAm–HPMACys triblock copolymer (abbreviated as PNC) consisting of a 10 kDa PEG mid block flanked by random blocks of NIPAAm and HPMACys with a feed ratio of 93 : 7 mol% of NIPAAm:HPMA-Cys was synthesized as previously reported.[34] Briefly, a PEG ABCPA macroinitiator, NIPAAm and HPMA-Boc-Cys(Acm) were dissolved in dry acetonitrile at a PEG:monomer ratio of 1 : 322, stirred for 48 h at 70 °C under a N_2 atmosphere and the polymer was subsequently collected after precipitation in diethyl ether. The Boc and Acm protecting groups on cysteine were removed by TFA and iodine treatment respectively.[34] In detail, a 3 g polymer was dissolved in DCM/TFA (1 : 1 v/v, 40 mL), stirred for 2 h, concentrated under reduced pressure and precipitated in diethyl ether. Next, the polymer was dissolved in MeOH/H_2O (1 : 1 v/v, 100 mL), followed by the addition of 1 mL 1 M HCl and 16 mL 0.2 M iodine in MeOH/H_2O (1 : 1 v/v). The mixture was stirred for 1 h at room temperature under a N_2 atmosphere, after which the excess of iodine was quenched with a few drops of 1 M ascorbic acid. Subsequently, the polymer in 100 mL MeOH/H_2O was treated with 1 g TCEP for 16 h to reduce disulfide bonds, purified by dialysis and lyophilized. The obtained protected and deprotected PNC polymers were characterized by ^{1}H NMR and deprotected PNC was also characterized by GPC. PNC protected: yield 88%, 1H NMR ($CDCl_3$): 3.97 (s, NIPAAm), 3.80 (t, terminal CH_2 PEG), 3.62 (m, CH_2 PEG backbone), 1.42 (s, Boc HPMA-Cys), 1.11 (s, NIPAAm). PNC deprotected: yield 62%, ^{1}H NMR (CDCl3): 3.97 (s, NIPAAm), 3.80 (t, terminal CH_2 PEG), 3.62 (m, CH_2 PEG backbone), 1.11 (s, NIPAAm). GPC: M_n = 43.0 kDa, M_w/M_n = 2.36.

2.3 Synthesis of a PEG 8-arm NHS cross-linker

PEG 20 000 8-arm was functionalized with N-hydroxysuccinimide (NHS) groups in a two step procedure according to literature procedures.[21] Briefly, a PEG 20 000 8-arm (10 g, 4 mmol OH terminal groups), glutaric anhydride (2.27 g, 20 mmol) and pyridine (1.6 mL) were dissolved in 20 mL chloroform and refluxed at 80 °C for 24 hours under a N_2 atmosphere. Methanol (100 mL) was added and the polymer was precipitated in 500 mL cold diethyl ether. The product was collected after filtration as a white powder and further dried under vacuum. Then, 10 g glutaric acid terminated PEG was dissolved in 50 mL DMSO together with NHS (4.4 g, 38 mmol) and EDCI (7.3 g, 38 mmol) and stirred for 1 h at room temperature. Subsequently, methanol (100 mL) was added and the product was collected as a white powder after precipitation in diethyl ether and filtration. Yield: 85%, degree of substitution (DS): 92%, ^{1}H NMR (CDCl3): δ = 4.24 (2H, t, terminal PEG CH_2), 3.62 (PEG backbone), 2.84 (4H,m, $2CH_2$ NHS), 2.71 (2H, t, $NOC(O)CH_2$), 2.49 (2H, t, $NOC(O)CH_2CH_2CH_2$), 2.06 (2H, p, $NOC(O)CH_2CH_2$).

2.4 Synthesis of a HA–NHS cross-linker

Hyaluronic acid (HA) was partially functionalized with N-hydroxysuccinimide (NHS) groups following a literature procedure.[38] In short, 1.0 g of hyaluronic acid (33 kDa) was dissolved in 30 mL PBS. NHS (1.6 g, 14 mmol) and EDCI (1.43 g, 7.4 mmol) were added

and the mixture was stirred for 2 h at room temperature. Next, the polymer was precipitated in cold ethanol (−20 °C) and centrifuged for 10 minutes at 7000 min^{-1} at 0 °C. This procedure was repeated twice and the HA–NHS product was collected as a white solid and further dried under vacuum. The ^{1}H NMR spectrum was recorded to calculate the degree of substitution (DS), defined as the number of NHS moieties per 100 disaccharide units. Yield: 93%, degree of substitution (DS): 38%, ^{1}H NMR (D_2O): δ = 4.6–3.3 (protons of HA), 2.79 (CH_2 of NHS), 2.00 ($NHC(O)CH_3$).

2.5 Synthesis of pHMGCL–NHS

Poly(hydroxymethylglycolide)-co-ε-caprolactone (pHMGCL) containing 8 mol% HMG groups (3.5 g, 2.2 mmol OH groups) was dissolved in 20 mL chloroform. Glutaric anhydride (1.1 g, 9.6 mmol) and pyridine (0.8 mL) were added and the mixture was refluxed for 24 h at 80 °C. Next, the mixture was cooled to room temperature and the polymer was precipitated in cold methanol (500 mL). The polymer derivatized with glutaric acid groups (pHMGCL-glut) was collected as a white solid after filtration. The obtained pHMGCL-glut (3.4 g) was dissolved in 30 mL chloroform and DCC (2.06 g, 10 mmol), DPTS (147 mg, 0.5 mmol) and NHS (1.15 g, 10 mmol) were added. The mixture was stirred for 3 h at room temperature. Next, dicyclohexyl urea (DCU) was removed by filtration and the obtained polymer was precipitated twice in cold methanol. The product was collected after filtration as a white solid and further dried under vacuum. pHMGCL–NHS was characterized by GPC, ^{1}H NMR and DSC.

Yield: 95%, molar ratio NHS/CL: 8/92, ^{1}H NMR (CDCl3): δ = 1.2–1.4 (m, $CH_2CH_2CH_2CH_2CH_2$), 1.5–1.7 (m, $C(O)CH_2CH_2CH_2$-CH_2CH_2), 2.1 (m, $CH_2CH_2CH_2C(O)ON$), 2.3 (t, $C(O)CH_2CH_2CH_2$-CH_2CH_2), 2.6–2.8 (m, $CH_2CH_2CH_2C(O)ON$), 2.8 (t, $NC(O)CH_2CH_2$), 4.1 (t, $C(O)CH_2CH_2CH_2CH_2CH_2$), 4.2–4.3 (m, CH–CH_2), 4.4–4.8 (m, $OCH_2C(O)$), 5.2–5.5 (m, *CH).*

2.6 Polymer characterization

The obtained polymers were characterized by gel permeation chromatography (GPC) and NMR spectroscopy. The molecular weight of PNC was determined by GPC using a PLgel 5 mm MIXED-D column (Polymer Laboratories) and a Waters 2414 refractive index detector. The column temperature was set at 65 °C and DMF containing 10 mM LiCl was used as an eluent. The elution rate was 1 mL min^{-1} and the sample concentration was 5 mg mL^{-1}. Calibration was performed using poly(ethylene glycol) standards of narrow and defined molecular weights.

The molecular weights of pHMGCL and pHMGCL–NHS were determined by GPC using a PL-gel 5 mm MIXED-D column and a Waters 2414 refractive index detector. AR grade THF was used as an eluent with a 1 mL min^{-1} flow rate at 30 °C. Polystyrene standards of known molecular weight were used for calibration.

The polymers were further characterized by ^{1}H NMR spectroscopy on an Agilent 400 MHz spectrometer. Chemical shifts are referred to the residual solvent peak (δ = 7.26 ppm for CDCl3 and 4.79 ppm for D_2O).

Europe PMC Funders Author Manuscripts

The thermal properties of the thermoplastic polymers were analyzed by DSC using a TA Instruments DSC Q2000 apparatus. Scans were taken from −80 °C to 100 °C with a heating rate of 10 °C min^{-1} and a cooling rate of 0.5 °C min^{-1} under a nitrogen flow. The glass transition temperature (T_g) was recorded in the second heating run as the midpoint of heat capacity change. Melting temperature (T_m) and the heat of fusion (ΔHf) were determined from the onset of the endothermic peak and the integration of endothermic area in the second heating run, respectively.

2.7 Rheological characterization

Rheological analysis of polymer solutions and hydrogels was performed on a Discovery HR-2 rheometer (TA Instruments, New Castle, DE, USA), using a 20 mm steel cone (1°) geometry equipped with a solvent trap. Flow and elastic properties of the polymer solutions and hydrogels were analyzed under similar conditions to those used during the 3D-printing process. Time sweeps were performed for 30 min at 20 °C, immediately followed by 3 h at 37 °C. Oscillation was performed at a frequency of 1 Hz and a strain of 1%, previously determined to be within the viscoelastic region of these hydrogels.[34]

To evaluate the effect of shear on the hydrogels similar to the shear experienced during printing, 30 min pre-crosslinked hydrogels were subjected to an increasing shear rate of 1 to 1000 s^{-1} at 20 °C under flow conditions. Strain recovery of the 30 min pre-crosslinked hydrogels was tested by applying 4 consecutive times a 3 minute logarithmic increase of the strain rate from 0.001 to 1000 s^{-1} at 20 °C under oscillation conditions and the effect of strain on viscosity, and storage and loss modulus was analyzed.

2.8 3D-printing of hydrogels

Hydrogels were printed using a 3D Discovery Printer and BioCAD software (RegenHU, Villaz-St-Pierre, Switzerland). A solution of PNC was shortly mixed for 1 minute with a solution of PEG–NHS or HA–NHS, to a total concentration of 7.5–3.8 wt% PNC–PEG or 7.5–1.6 wt% PNC–HA, and transferred into a 3 or 10 mL syringe. The polymeric solutions were allowed to pre-crosslink for 30 min before starting filament deposition. A pressure of 3–4 bar was applied for pneumatic extrusion. A printing head movement speed in the *x* and *y* plane (F_{xy}) of 5 mm s^{-1} and a layer height of 0.25 mm were used. Nordson EFD (Westlake, Ohio, USA) dispensing SmoothFlow tapered tips with an inner nozzle diameter of 0.25 mm was used that matched with the high solution viscosity. 3D-printing was performed using a heated plate of 37–40 °C. A red food coloring agent, Ponceau 4R, E number 124 was added to the HA–NHS solution in a concentration of 50 mL coloring agent per 1 mL HA solution to obtain additional visual contrast that allowed accurate evaluation of the porosity. Hydrogel porosity of the 3D-printed condyle shape PNC–PEG constructs was estimated after measuring the construct dimensions and weighing the construct, using the following equation:

$$\left(1-\frac{\text{hydorgel weight(mg)}}{\text{hydrogel volume}(\text{mm}^3)}\right)\times 100\%$$

Europe PMC Funders Author Manuscripts

2.9 3D-printing of NHS functionalized thermoplastic polymers

Thermoplastic pHMGCL–NHS constructs were printed using a BioScaffolder dispensing system (Sys + Eng, Salzgitter-Bad, Germany). Cylindrical scaffolds (diameter: 15 mm, height: 0.9 mm, strand spacing 1.5 mm, 5 layers) were designed with Rhino 3D software (McNeel, Seattle, WA, USA) and the Standard Tessellation Language (STL) file of this model was translated to g-code and executed on a BioScaffolder with computer-aided manufacturing (CAM) software (PrimCAM, Einsiedeln, Switzerland).[33] pHMGCL–NHS was melted at 140 °C for extrusion through a 25G metal needle (DL Technology LLC, Haverhill, MA, USA). A pressure of 0.4 MPa was applied, followed by screw-driven extrusion at a deposition speed of 250 mm min^{-1}. The BioScaffolder was placed within a laminar flow cabinet to ensure the rapid solidification of the printed fibers.

2.10 Dynamic mechanical analysis

Cylindrically shaped PNC–PEG hydrogels of 7.5–3.8 wt% with a volume of 100 mL were prepared in plastic molds with a diameter of 4 mm. Reinforced pHMGCL–NHS – PNC–PEG materials were prepared after filling the pores of constructs described in Section 2.9 with a PNC–PEG hydrogel. The Young's moduli of these constructs were determined on a Q800 DMA (TA Instruments, New Castle, DE, USA) in triplicate after 3 hour cross-linking at 37 °C. Compression from 0.01 till 0.1 N with a rate of 0.01 N min^{-1} was applied to the hydrogels and from 0.01 to 5 N with a rate of 0.5 N min^{-1} to the reinforced constructs at room temperature. The Young's modulus was determined from the first linear region of the stress–strain curve.

2.11 Creep-recovery test: interface-grafting strength

The effect of grafting of PNC–PEGNHS and pHMGCL–NHS was investigated in creep-recovery tests that were performed using a Discovery HR-2 rheometer (TA-instruments), similar to previously described methods.[33] Flat discs (surface area 80 mm^2, thickness 0.1 mm) of pHMGCL and pHMGCL–NHS were prepared after dissolving the polymer in chloroform (160 mg mL^{-1}) and depositing droplets on a glass petri dish, subsequently allowing the chloroform to evaporate overnight. PEG–NHS and PNC solutions in PBS were prepared at 4 and 15 wt% concentrations, respectively, 4 hours before starting the experiment. Measurements were performed in triplicate. The pHMGCL or pHMGCL–NHS discs were attached with a photosticker (HEMA, Groningen, the Netherlands) to the upper 40 mm diameter plate of the geometry. PEG–NHS (50 μL*)* was mixed with PNC (50 mL*)* and pipetted on the bottom plate before lowering the top plate to a gap of 1.0 mm at which the hydrogel and thermoplastic had a narrow surface interface. The construct was allowed to crosslink for 3 hours at 37 °C. Next, the obtained constructs were mechanically deformed at different torque values ranging from 100 to 1000 mNm, using a step-wise increase of 100 mNm. This deformation consisted of a 1 minute creep followed by 1 minute recovery, while keeping the temperature at 37 °C. In the creep step, a constant torque force was applied on the top thermoplastic layer that was in contact with the hydrogel and the observed strain or deformation of the material was recorded over time. In the recovery step, the applied force was released, and the construct was allowed to recover to the starting position. The torque

value at which the deformation resulted in detachment of the hydrogel and thermoplastic was noted as the construct failure.

2.12 Live/dead viability

A Live/dead viability assay (calcein AM/ethidium homodimer, Life Sciences, USA) was performed on the reinforced pHMGCL–NHS – PNC–PEG and pHMGCL–NHS – PNC–HA constructs, as previously described[14,39] and according to recommendations of the manufacturer. Briefly, chondrocytes were harvested from full thickness cartilage of an equine stifle joint, after consent of the owner of the horses, according to previously published procedures.[39] Chondrocytes were encapsulated in the hydrogels at passage 2 at a concentration of 5×10^6 cells per mL. Hydrogels containing cells were allowed to form for 1.5 h at 37 °C before culture medium was added. Viability of the chondorocytes was visualized using a light microscope (Olympus, BX51, USA) with excitation/emission filters set at 488/530 nm and 530/580 nm to detect living (green) cells and dead (red) cells respectively after 1.5 h. Live and dead cells were counted for two samples per group at four locations within the construct. Cell viability was calculated using the following equation:

$$\frac{\text{live cells}}{\text{total cells}} \times 100\%$$

2.13 Histology

Constructs that were previously analyzed with a live/dead assay were fixed in formalin for histological examination. The samples were dehydrated through a graded ethanol series, cleared in xylene and embedded in paraffin. The samples were subsequently sectioned and stained with hematoxylin and eosin (H&E) to visualize cell distribution in the reinforced constructs.

2.14 Statistics

Construct failure data from creep-recovery experiments, Young's modulus data from DMA measurements and cell viability data were assessed by a Mann-Whitney-U test, using GraphPad Prism 6 software (La Jolla, Ca, USA). A p o 0.05 was considered as significant.

3 Results and discussion

3.1 Hydrogel components

Polymer structures of the hydrogel building blocks used in this study and the OMNCL mechanism are shown in Fig. 1. The triblock copolymer PEG–NIPAAm–HPMACys (PNC) was synthesized by radical polymerization and consisted of a PEG 10 kDa midblock, flanked by 20 kDa random blocks of NIPAAm and HPMA-cysteine. NIPAAm was introduced for its thermosensitive characteristics, while cysteine functionalities enable covalent chemical cross-linking.[34] The obtained molar ratio of NIPAAm : cysteine in the PNC polymer was 94 : 6 according to NMR analysis, which is in good agreement with the feed ratio (93 : 7). This polymer exhibited a lower critical solution temperature (LCST) of 30 °C in water, hence behaving as a liquid solution at room temperature and forming a physically cross-linked network above its LCST.[34]

Europe PMC Funders Author Manuscripts

Poly(ethylene glycol) (PEG) 8-arm and hyaluronic acid (HA) cross-linkers were functionalized with N-hydroxysuccinimide (NHS) groups with a degree of substitution (DS) of 92% and 38% respectively as determined by ^{1}H NMR. DS is defined as the percentage of PEG hydroxyl or HA carboxylic acid groups that were converted into NHS moieties. The NHS functionalized polymers were purified by precipitation instead of dialysis, to limit potential premature hydrolysis of the NHS ester bonds.

3.2 3D-printing and rheological assessment

A few requirements were listed to achieve optimal 3D-printing based on previous experience and the experiments reported by Rutz *et al.* [24] Firstly, we aimed for a maximal pre-crosslinking time of 30 minutes before starting extrusion, since a long waiting time can have negative effects on cells that can be entrapped in the hydrogel. Secondly, the hydrogel should be deposited as an intact filament with sufficient yield stress and without collapse on the printing plate. Therefore, polymer concentrations of the aqueous solutions were optimized to allow extrusion of gel filaments without filament fracturing or clogging the nozzle while maintaining high shape fidelity. It was found that hydrogel concentrations above 25 wt% were deposited as lose fractions instead of intact filaments, thereby creating structures with low shape fidelity as well as quick nozzle obstruction. In contrast, hydrogels with a total polymer concentration below 8 wt% required pre-crosslinking times of more than 30 minutes before allowing extrusion without a collapse of the construct.

Therefore, hydrogel concentrations of 7.5 wt% PNC mixed with 3.8 wt% PEG–NHS (total polymer conc. 11.3 wt%) or 7.5 wt% PNC mixed with 1.6 wt% HA-NHS (total polymer conc. 9.1 wt%), both corresponding to a 1 : 1 functional group ratio, were chosen for creating structures with both good shape fidelity as well as maintaining filament extrusion. These concentrations were significantly lower than the concentrations needed for 3D-printing of similar thermosensitive hydrogels without partial pre-cross-linking (≥25 wt%).[14,16] Furthermore, pre-crosslinking times were significantly shorter than previously reported for partially cross-linked hydrogels when extrusion was performed after 2 hours, as a result of the efficient chemical cross-linking using oxo-ester mediated native chemical ligation.[24]

An anatomically relevant model of a femoral condyle was created and printed using PNC–PEG hydrogel formulations (Fig. 2). Three dimensional structures were created by depositing multiple layers while retaining the shape of the hydrogel (Fig. 2C and D). The 3D-printed PNC–PEG hydrogels exhibited an average porosity of 47.9 ± 2.3%. Creating porous networks is extremely important for facilitating nutrient diffusion, tissue contact and tissue ingrowth.[15,40]

The shape maintaining properties of these hydrogel filaments were further illustrated by the creation of a hollow cone model (Fig. 2E). Filaments were deposited onto constructs with an angle of approximately 45°, thereby creating overhang geometries without the necessity of an external support material. Furthermore, porous grid-like constructs of PNC–HA hydrogels were created (Fig. 2G and H), showing the possibility to create specific internal gaps that can enhance the diffusion of nutrients through the construct. Overall, there were no clear differences in the possibility to extrude PNC–PEG and PNC–HA hydrogels. However, as a result of the fast cross-linking kinetics of PNC–HA hydrogels it was important to

quickly transfer the solutions to the syringe, while still ensuring homogeneous mixing of the two components and avoiding the presence of air bubbles in the mixture, since this hampers the extrusion of continuous, cohesive filaments.

Interestingly, the 3D-printing window, defined as the time frame when it was possible to print the polymer solutions, was not as narrow as previously described for partially cross-linked two-component materials.[1,24] Even after two hours of pre-crosslinking in the syringe, the hydrogels could still be extruded and deposited with the same shape fidelity. Extrusion was possible by increasing the pressure from 3 to 4 bar over time, and continuous extrusion was achieved for the fabrication of a construct of approximately 20 cm^3 during 1 hour. Alternatively, these hydrogels may be attractive for printing with a dual extrusion nozzle. The use of a dual syringe printing head can eliminate the change in viscosity during 3D-printing, since the two components will only be mixed shortly prior to deposition. However, besides the difficulties to allow proper mixing, very fast gelation needs to be ensured to allow the formation of constructs with high shape fidelity. Therefore, this approach may be less feasible for 3D-printing of hydrogels with a relatively low polymer content.

The mechanical and flow properties of the gels were evaluated by rheology experiments, since control over flow properties is one of the major characteristics for successful translation into a 3D-printed construct.[1] In our strategy, four relevant steps of 3D-printing were identified. In the first step, the hydrogels are left in the syringe at room temperature, allowing them to partially cross-link. This step was imitated during rheology experiments by using limited oscillation of 1% strain and 1 Hz frequency at 20 °C and analyzing the evaluation of storage and loss moduli (G^0 and G^{00}) in time. In the second step, the hydrogel is extruded through the nozzle, which was characterized as a shear rate ramp. In the third and fourth step, the partially cross-linked hydrogel is deposited on a 37 °C plate and subsequently allowed to further harden in time. This last part was imitated by increasing the temperature during rheology measurements to 37 °C and again applying minimal oscillation. As depicted in Fig. 3A and B, G^0 and G^{00} were measured for 30 minutes at 20 °C, followed by 3 hours at 37 °C. At room temperature, the PNC–PEG aqueous systems showed an increase in G^0 resulting in a higher value of G^0 compared to G^{00} after 10 minutes (ESI,† Fig. S1), thereby going from fluid-like (viscous) to viscoelastic behavior. In contrast, the PNC–HA mixtures already showed this transition immediately upon starting the rheological measurement. The more rapid gelation of PNC–HA can be ascribed to the higher amount of NHS functionalities per HA chain in comparison to PEG and is in line with previous work.[34] To explain, with a DS of 38% and a molecular weight of 33 kDa, HA had on average 32 NHS moieties per chain, compared to only 7.4 NHS moieties on PEG. After 30 minutes of cross-linking PNC–PEG reached a storage modulus of 0.7 kPa, while PNC–HA reached a G' of 2.1 kPa.

Subsequently, the temperature was increased to 37 °C, mimicking the temperature change during deposition on a heated plate. The storage moduli increased immediately to 1.2 kPa and 3.3 kPa for PNC–PEG and PNC–HA, respectively, as a result of the thermoresponsive properties of the polymers. The ~1.6 fold increase in G' resulted in an immediate extra stabilization of the hydrogel network. Rheology measurements also showed a more rapid increase in G' after raising the temperature likely as a result of the increased kinetics of the

OMNCL reaction at 37 °C. After an additional 3 hours of network formation, both formulations reached a storage modulus of approximately 9 kPa. A similar storage modulus for both formulations was expected based on a comparable polymer concentration in both hydrogel formulations and an equal functional group content. Furthermore, the flow properties of the hydrogels as experienced during the actual extrusion through the nozzle were studied by rheology. After increasing the shear rate (Fig. 3C), a decrease in viscosity was observed, similar to the shear-thinning or pseudoplastic behavior that is often encountered for polymeric solutions.[42] Importantly, as depicted in Fig. 3D, the process of increasing and decreasing strain that was applied on the hydrogel could be repeated several times, thereby proving that the hydrogel structure remained intact and recovered rapidly. At each step, the storage modulus and viscosity at low shear increased compared to the previous step, showing that the cross-linking continued in time. Based on the used needle diameter (d) of 0.25 mm and a printing velocity *(v)* of 5 mm s^{-1}, the estimated shear rate ($\dot{\gamma}$) in the needle was calculated using the equation: $\dot{\gamma} = \frac{8v}{d}$, which corresponded to 160 s^{-1}.[43] Here, we assumed that the printing velocity matches the velocity in the needle. At this shear rate, the partially cross-linked hydrogels had a low viscosity of 5.4 Pa s for PNC–PEG and 2.5 Pa s for PNC–HA (Fig. 3C). Additionally, the hydrogels showed a sudden collapse in viscosity at a strain rate of approximately 12 s^{-1} (ESI,† Fig. S3C). These viscosity profiles confirm that with our 3D-printing approach the hydrogels were moldable, thereby making it possible for the gels to be extruded through a small needle. It must be noted that during extrusion, shear forces exerted on the hydrogel are maximal near the wall instead of homogenously as during the rheology experiments, hence minimally influencing the hydrogel structure in the middle of the nozzle. Rutz *et al.* [24] previously suggested that the extrusion of partially cross-linked hydrogels was likely facilitated by the localized rupture of the gel at the wall of the nozzle, thereby facilitating the extrusion of continuous cohesive filaments.

3.3 Reinforced hydrogel–thermoplastic constructs

To increase the mechanical strength of the 3D-printed hydrogels, multi-material constructs were formed by combining the hydrogel with a thermoplastic polyester. To this end, an NHS-functionalized thermoplastic polymer, abbreviated as pHMGCL–NHS, was successfully synthesized and characterized to enable the formation of covalent grafting with the hydrogel, thereby allowing optimal material integration.

The thermoplastic polymer pHMGCL contained 8% HMG groups, defined as the molar ratio HMG/CL. The OH groups of HMG were fully functionalized with NHS groups in a two-step reaction. Successful functionalization is shown by ^{1}H NMR spectroscopy (Fig. 4). The polymers are abbreviated as pHMGCL and pHMGCL–NHS for the polymers with and without NHS functionalities, respectively, and the polymer characteristics are listed in Table 1.

Analysis of the number average molecular weight (M_n) by GPC showed a slight increase from 16.3 to 17.9 kDa after functionalization with NHS groups, indicating that neither premature cross-linking nor chain scission had occurred during the synthesis. Additionally, the thermal properties of the obtained polymers were evaluated with DSC. Both pHMGCL and pHMGCL–NHS displayed semi-crystalline thermoplastic behavior with a low T_g of −47

and −38 °C, respectively, and a melting temperature (T_m) of around 50 °C. The increase in T_g after NHS functionalization was ascribed to the lower mobility of the polymer chains as a result of the bulky NHS groups.

Reinforced thermoplast–hydrogel constructs were fabricated as depicted in Fig. 5 from a cylindrical porous scaffold. To obviate the difficulties of simultaneously 3D-printing hydrogel–thermoplastic constructs, in this study the hydrogel was casted in the pores of the 3D-printed thermoplastic construct, which ensured proper integration between the different materials. Pores filled with hydrogel were created with a size of 1.1 ± 0.4 mm, which is in good agreement with the 1.5 mm strand spacing of the designed model. Pores were of sufficient size to increase mechanical strength without limiting cell migration in the hydrogel.[44] The Young's modulus increased from 17 ± 1 kPa for only hydrogel based constructs to 645 ± 12 kPa for reinforced hydrogels, a 38 fold increase (Fig. 5C). Importantly, the mechanical strength of the reinforced construct was similar to the thermoplastic construct alone (814 ± 75 kPa), thereby primarily dependent on the thermoplastic properties. "During the construct fabrication and measurement, limited degradation and swelling of the hydrogel–thermoplastic construct was expected. A lower Young's modulus of the hydrogel–thermoplastic construct could be caused by inconsistency in the geometry during fabrication of the construct. Additionally, a layer of mechanically weak hydrogel on top of the thermoplastic could have influenced the Young's modulus measurement".

It is expected that the mechanical strength of the reinforced constructs can be further tailored by altering the construct geometries, such as the fiber distance and fiber diameter.[45]

To gain insight into whether the hydrogel is indeed covalently grafted to the thermoplastic support material, the functional group ratio of NHS : cysteine at the thermoplast–hydrogel interface was calculated. To this end, the amount of functional groups per volume was calculated where we assumed that all functional groups were equally distributed over the materials (i.e. the same density of functional groups at the interface and the bulk). The amount of functional groups per volume present on the thermoplastic polymer was estimated using the mass percentage of functional groups in the thermoplastic polymer and the density of the polymer. This was compared to the number of available cysteine groups, using the polymer concentration in the hydrogel. On average, the thermoplastic polymer pHMGCL–NHS has 22 times more functional groups per volume (and thus also at the interface) compared to the number of cysteine moieties in the used hydrogel. Therefore, it can be expected that there are plenty of NHS groups on the thermoplastic polymer available for cross-linking with the cysteine moieties in the hydrogel. This material integration was tested in a creep-recovery experiment by applying friction at the material interface (Fig. 6). For this, a cysteine : NHS functional group ratio of 2 : 1 was used in the hydrogel to ensure that remaining cysteines were available for cross-linking with the thermoplastic. In a creep-recovery experiment, a stepwise increased torque force, followed by a 1 minute recovery, was applied on top of the thermoplastic. The moment that the thermoplastic was disintegrated from the hydrogel was characterized by high strain values and a lack of strain recovery. The corresponding torque force was assigned as the point of construct failure. As shown in Fig. 6C, PNC–PEG hydrogels combined with pHMGCL–NHS exhibited a

significantly 1.6 fold higher resistance against rotational friction compared to hydrogels combined with the thermoplastic without NHS groups (pHMGCL). Therefore, it can be concluded that the functional NHS groups in the thermoplastic contributed to a higher material integration, similar to what has been found previously for photopolymerized constructs.[33]

Although the measurements were already performed after 3 hours to limit water evaporation, it is expected that this integration will further increase in time, since it was previously shown that the chemical cross-linking was not completed after 3 hours.[22]

Chondrocytes were embedded in the reinforced thermoplast–hydrogel construct to investigate the cytocompatibility of the cells in the hydrogel. Since the polymer solutions had a low viscosity prior to mixing of the two components, chondrocytes were easily and homogeneously mixed with the PNC solution and then added to the PEG or HA solution. Cell viability was analyzed after 1.5 hours for a reinforced pHMGCL– NHS network covalently grafted to a hydrogel containing PNC–PEG or PNC–HA (Fig. 7A and B) to analyze the effect of initial cross-linking on cell viability. Since there were no clear differences in chondrocyte cell viability in the hydrogels after 4 hours or 7 days of culture (ESI,† Fig. S2), an early time point of 1.5 h was used to analyze the differences in cell viability between PNC–PEG and PNC–HA reinforced constructs. The reinforcing thermoplastic fibers are shown in white, with hydrogel containing chondrocytes homogeneously distributed in the pores. Cell viability was significantly higher for the constructs containing hyaluronic acid (90 ± 9%) compared to constructs containing PEG (43 ± 23%), as was expected since PEG is a biologically inert material and lacks adhesion sites. Several studies have shown the potential of hyaluronic acid to induce matrix formation by embedded cells, thereby making it an attractive biomaterial.[46–49] The same viability results were obtained for the hydrogels as such, proving that the thermoplastic network did not adversely affect the viability of the entrapped cells.

The cell distribution was analyzed by histology using a hematoxylin and eosin (H&E) staining. Cells were homogeneously distributed in the PNC–PEG hydrogel (Fig. 7C and D). Importantly, histological analysis showed that cells were also located near the thermoplastic fibers, thereby showing no deleterious effects on the presence of the thermoplastic polymer strands, in line with previous studies.[33] Similar results of cell distribution were obtained for the PNC–HA reinforced constructs (data not shown). Taken together, these results showed that chondrocytes can be easily and homogeneously incorporated into the reinforced constructs and showed a favorable cell viability in the constructs containing hyaluronic acid.

4 Conclusion

This study describes the development of a novel bioink from a partially cross-linked, yet extrudable and self-supporting hydro-gel. The hydrogels were chemically cross-linked by oxo-ester mediated native chemical ligation and physically cross-linked after deposition on a 37 °C printing plate as a result of their thermoresponsive properties. Further, mechanical strength was greatly enhanced after covalent grafting to a thermoplastic polymer scaffold. The bioinks described in this study provide new possibilities for biofabrication, given their

versatility in mechanical properties, high construct integrity and controllable 3D-printing as supported by rheology.

Supplementary Material

Refer to Web version on PubMed Central for supplementary material.

Acknowledgements

This work was supported by a grant from the Dutch government to the Netherlands Institute for Regenerative Medicine (NIRM, grant no. FES0908) and the Dutch Arthritis Foundation. Part of the research leading to these results has received funding from the European Union Seventh Framework Programme (FP7/2007-2013) under grant agreement no. 309962 (HydroZones) and from the European Research Council under grant agreement no. 647426 (3D-JOINT).

References

1. Malda J, Visser J, Melchels FP, Jüngst T, Hennink WE, Dhert WJA, Groll J, Hutmacher DW. Adv Mater. 2013; 25:5011–5028. [PubMed: 24038336]
2. Skardal A, Atala A. Ann Biomed Eng. 2015; 43:730–746. [PubMed: 25476164]
3. Melchels FP, Feijen J, Grijpma DW. Biomaterials. 2010; 31:6121–6130. [PubMed: 20478613]
4. Melchels FPW, Domingos MAN, Klein TJ, Malda J, Bartolo PJ, Hutmacher DW. Prog Polym Sci. 2012; 37:1079–1104.
5. Fedorovich NE, Alblas J, de Wijn JR, Hennink WE, Verbout AJ, Dhert WJA. Tissue Eng. 2007; 13:1905–1925. [PubMed: 17518748]
6. Derby B. Science. 2012; 338:921–926. [PubMed: 23161993]
7. Kolesky DB, Truby RL, Gladman A, Busbee TA, Homan KA, Lewis JA. Adv Mater. 2014; 26:3124–3130. [PubMed: 24550124]
8. Klein TJ, Rizzi SC, Reichert JC, Georgi N, Malda J, Schuurman W, Crawford RW, Hutmacher DW. Macromol Biosci. 2009; 9:1049–1058. [PubMed: 19739068]
9. Buwalda SJ, Boere KWM, Dijkstra PJ, Feijen J, Vermonden T, Hennink WE. J Controlled Release. 2014; 190:254–273.
10. Peppas NA, Hilt JZ, Khademhosseini A, Langer R. Adv Mater. 2006; 18:1345–1360.
11. Seliktar D. Science. 2012; 336:1124–1128. [PubMed: 22654050]
12. Billiet T, Vandenhaute M, Schelfhout J, Van Vlierberghe S, Dubruel P. Biomaterials. 2012; 33:6020–6041. [PubMed: 22681979]
13. Kesti M, Müller M, Becher J, Schnabelrauch M, D'Este M, Eglin D, Zenobi-Wong M. Acta Biomater. 2015; 11:162–172. [PubMed: 25260606]
14. Censi R, Schuurman W, Malda J, Di Dato G, Burgisser PE, Dhert WJA, Van Nostrum CF, Di Martino P, Vermonden T, Hennink WE. Adv Funct Mater. 2011; 21:1833–1842.
15. Melchels FPW, Dhert WJA, Hutmacher DW, Malda J. J Mater Chem B. 2014; 2:2282–2289. [PubMed: 32261716]
16. Fedorovich NE, Swennen I, Girones J, Moroni L, Van Blitterswijk CA, Schacht E, Alblas J, Dhert WJA. Biomacromolecules. 2009; 10:1689–1696. [PubMed: 19445533]
17. Discher DE, Janmey P, Wang Y-l. Science. 2005; 310:1139–1143. [PubMed: 16293750]
18. Mironi-Harpaz I, Wang DY, Venkatraman S, Seliktar D. Acta Biomater. 2012; 8:1838–1848. [PubMed: 22285429]
19. Jiang Y, Chen J, Deng C, Suuronen EJ, Zhong Z. Biomaterials. 2014; 35:4969–4985. [PubMed: 24674460]
20. Wan Q, Chen J, Yuan Y, Danishefsky SJ. J Am Chem Soc. 2008; 130:15814–15816. [PubMed: 18855357]
21. Strehin I, Gourevitch D, Zhang Y, Heber-Katz E, Messersmith PB. Biomater Sci. 2013; 1:603–613. [PubMed: 23894696]

22. Boere KWM, van den Dikkenberg J, Gao Y, Visser J, Hennink WE, Vermonden T. Biomacromolecules. 2015; 16:2840–2851. [PubMed: 26237583]
23. Skardal A, Zhang J, McCoard L, Oottamasathien S, Prestwich GD. Adv Mater. 2010; 22:4736–4740. [PubMed: 20730818]
24. Rutz AL, Hyland KE, Jakus AE, Burghardt WR, Shah RN. Adv Mater. 2015; 27:1607–1614. [PubMed: 25641220]
25. Skardal A, Zhang J, McCoard L, Xu X, Oottamasathien S, Prestwich GD. Tissue Eng, Part A. 2010; 16:2675–2685. [PubMed: 20387987]
26. Schuurman W, Khristov V, Pot MW, Van Weeren PR, Dhert WJA, Malda J. Biofabrication. 2011; 3
27. Visser J, Peters B, Burger TJ, Boomstra J, Dhert WJA, Melchels FPW, Malda J. Biofabrication. 2013; 5
28. Visser J, Melchels FPW, Jeon JE, van Bussel EM, Kimpton LS, Byrne HM, Dhert WJA, Dalton PD, Hutmacher DW, Malda J. Nat Commun. 2015; 6
29. Woodruff MA, Hutmacher DW. Prog Polym Sci. 2010; 35:1217–1256.
30. Seyednejad H, Vermonden T, Fedorovich NE, van Eijk R, van Steenbergen MJ, Dhert WJA, van Nostrum CF, Hennink WE. Biomacromolecules. 2009; 10:3048–3054. [PubMed: 19807059]
31. Seyednejad H, Gawlitta D, Kuiper RV, de Bruin A, van Nostrum CF, Vermonden T, Dhert WJ, Hennink WE. Biomaterials. 2012; 33:4309–4318. [PubMed: 22436798]
32. Seyednejad H, Gawlitta D, Dhert WJA, Van Nostrum CF, Vermonden T, Hennink WE. Acta Biomater. 2011; 7:1999–2006. [PubMed: 21241834]
33. Boere KWM, Visser J, Seyednejad H, Rahimian S, Gawlitta D, van Steenbergen MJ, Dhert WJA, Hennink WE, Vermonden T, Malda J. Acta Biomater. 2014; 10:2602–2611. [PubMed: 24590160]
34. Boere KWM, Soliman BG, Rijkers DTS, Hennink WE, Vermonden T. Macromolecules. 2014; 47:2430–2438.
35. Hu B-H, Su J, Messersmith PB. Biomacromolecules. 2009; 10:2194–2200. [PubMed: 19601644]
36. Neradovic D, van Nostrum CF, Hennink WE. Macro-molecules. 2001; 34:7589–7591.
37. Moore JS, Stupp SI. Macromolecules. 1990; 23:65–70.
38. Chang CY, Chan AT, Armstrong PA, Luo H-C, Higuchi T, Strehin IA, Vakrou S, Lin X, Brown SN, O'Rourke B. Biomaterials. 2012; 33:8026–8033. [PubMed: 22898181]
39. Visser J, Levett PA, te Moller NCR, Besems J, Boere KWM, Van Rijen MHP, de Grauw JC, Dhert WJA, van Weeren R, Malda J. Tissue Eng. 2015; 21:1195–1206.
40. Hollister SJ. Nat Mater. 2005; 4:518–524. [PubMed: 16003400]
41. Iverson, C. The American Heritage[S] Dictionary of the English Language. Fifth edn. Houghton Mifflin Harcourt Publishing Company; 2015.
42. Guvendiren M, Lu HD, Burdick JA. Soft Matter. 2012; 8:260–272.
43. Darby, R. Chemical Engineering Fluid Mechanics. 2nd edn. Taylor & Francis; 2001.
44. Murphy CM, Haugh MG, O'Brien FJ. Biomaterials. 2010; 31:461–466. [PubMed: 19819008]
45. Moroni L, De Wijn JR, Van Blitterswijk CA. Biomaterials. 2006; 27:974–985. [PubMed: 16055183]
46. Yoo HS, Lee EA, Yoon JJ, Park TG. Biomaterials. 2005; 26:1925–1933. [PubMed: 15576166]
47. Baier Leach J, Bivens KA, Patrick CW Jr, Schmidt CE. Biotechnol Bioeng. 2003; 82:578–589. [PubMed: 12652481]
48. Collins MN, Birkinshaw C. Carbohydr Polym. 2013; 92:1262–1279. [PubMed: 23399155]
49. Levett PA, Melchels FP, Schrobback K, Hutmacher DW, Malda J, Klein TJ. Acta Biomater. 2014; 10:214–223. [PubMed: 24140603]

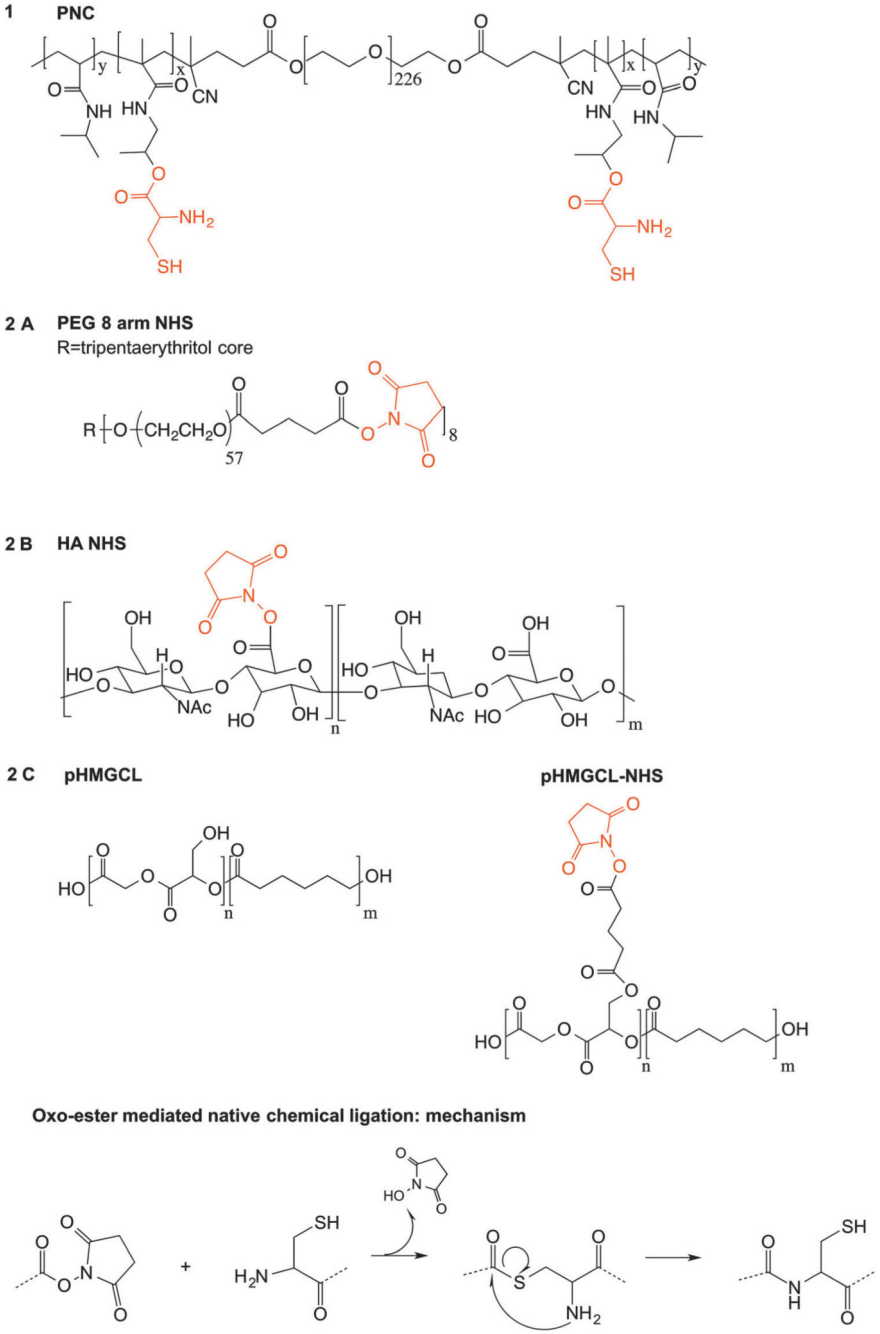

Fig. 1.

Overview of chemical structures of polymers used in this study and the chemical cross-linking mechanism (oxo-ester mediated native chemical ligation).

Europe PMC Funders Author Manuscripts

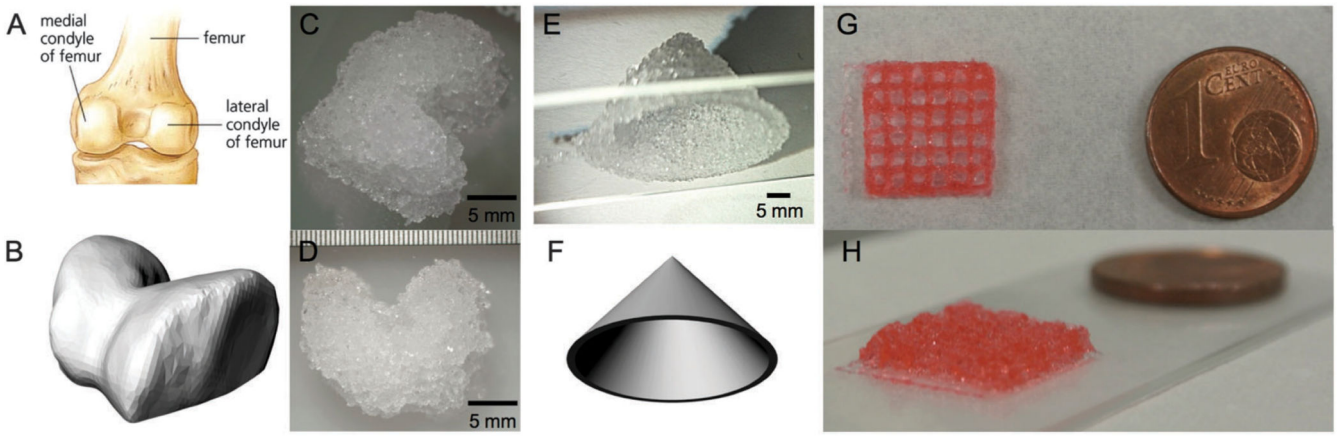

Fig. 2.

(A) Schematic display of femoral condyles, adapted from the American Heritage Dictionary.[41] (B) CAD model of femoral condyle. (C) and (D) 3D-printing of PNC–PEG NHS hydrogels in a condyle shape. (E) Hollow cone shape, showing the possibility to create overhangs without support. (F) CAD model of hollow cone. (G) and (H) 3D-printing of PNC–HA NHS hydrogels in porous grid shapes.

Europe PMC Funders Author Manuscripts

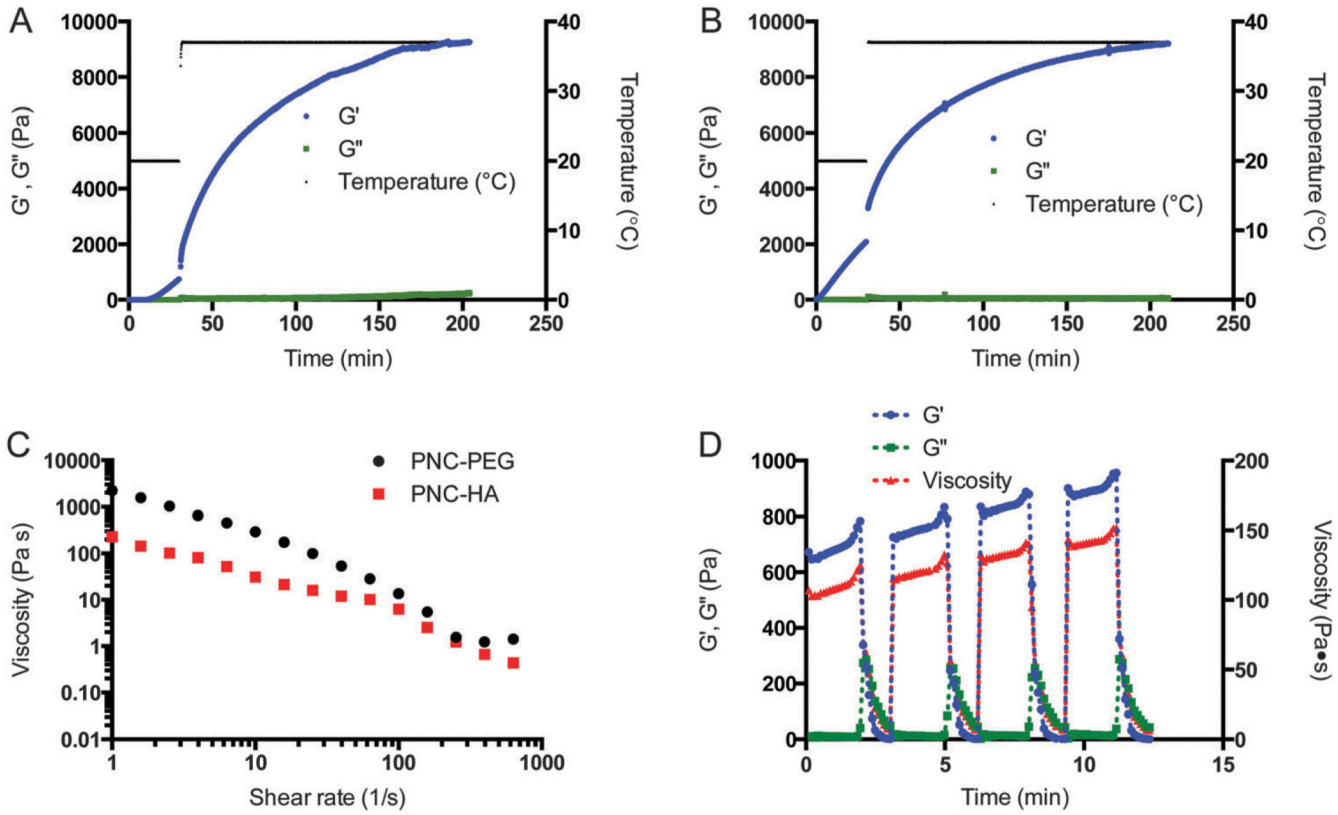

Fig. 3.

Rheological and flow characteristics of hydrogels imitating the hydrogel plotting process. (A) PNC–PEG 7.5–3.8 wt%, 30 min pre-crosslinking at 20 °C, 3 h measuring at 37 °C. (B) PNC–HA 7.5–1.6 wt%, 30 min 20 °C, 3 h 37 °C. (C) PNC–PEG and PNC–HA shear rate flow sweep, applied after 30 min at 20 °C. (D) Four oscillation strain ramps on PNC–PEG 7.5–3.8 wt% after 30 min at 20 °C to test hydrogel recovery. The strain rate was increased logarithmically from 0.001 to 1000 s^{-1} for 3 minutes.

Europe PMC Funders Author Manuscripts

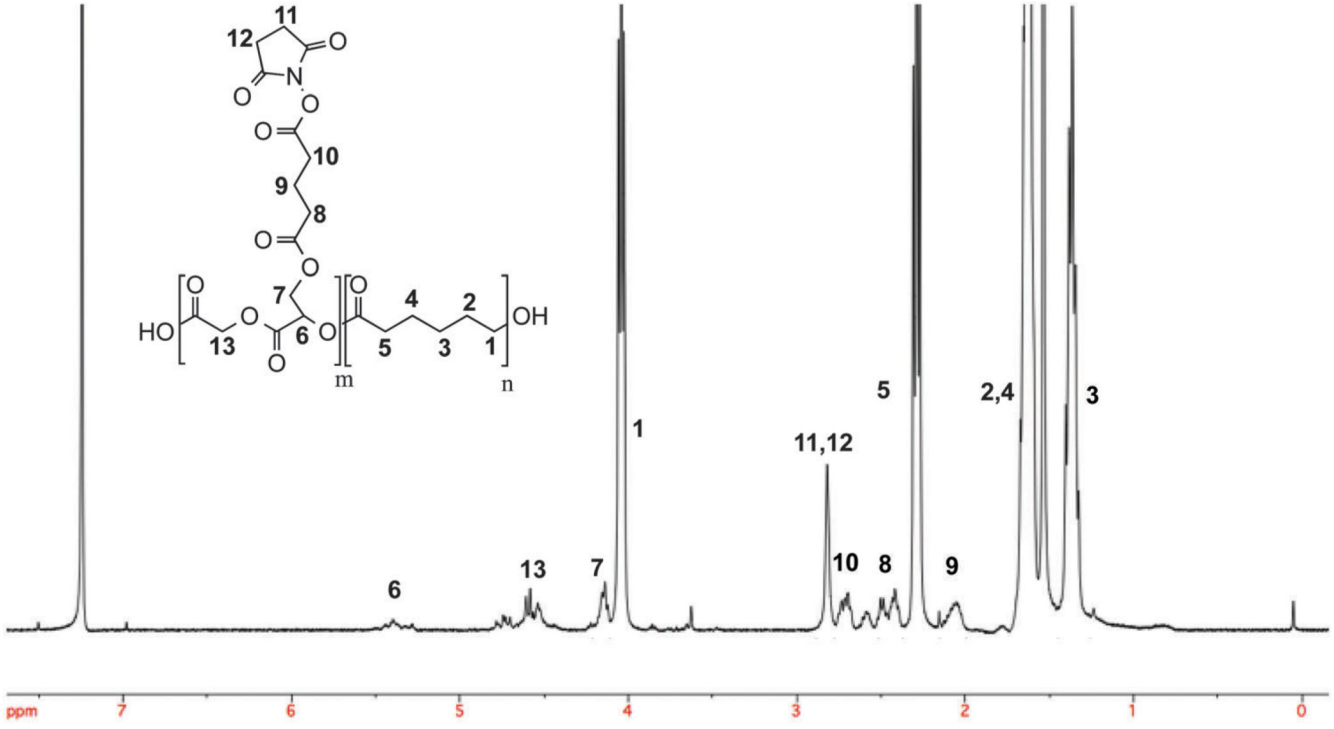

Fig. 4.

Chemical structure and ^{1}H NMR of NHS-functionalized thermoplastic pHMGCL–NHS in $CDCl_3$. Ratio NHS/CL = 8/92.

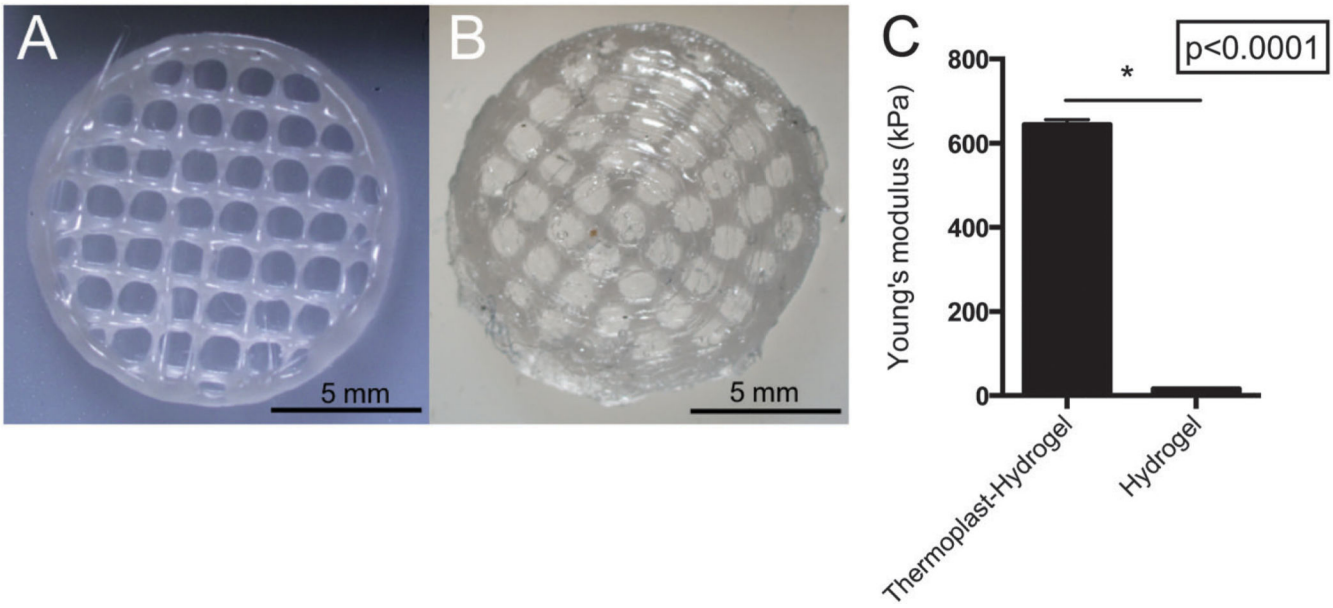

Fig. 5.

Reinforced thermoplast–hydrogel constructs. (A) pHMGCL–NHS 3D-printed network. (B) pHMGCL–NHS – PNC–PEGNHS thermoplast– hydrogel construct. (C) Young's modulus as measured by DMA of the PNC–PEG NHS hydrogel and reinforced thermoplast–hydrogel constructs.

Europe PMC Funders Author Manuscripts

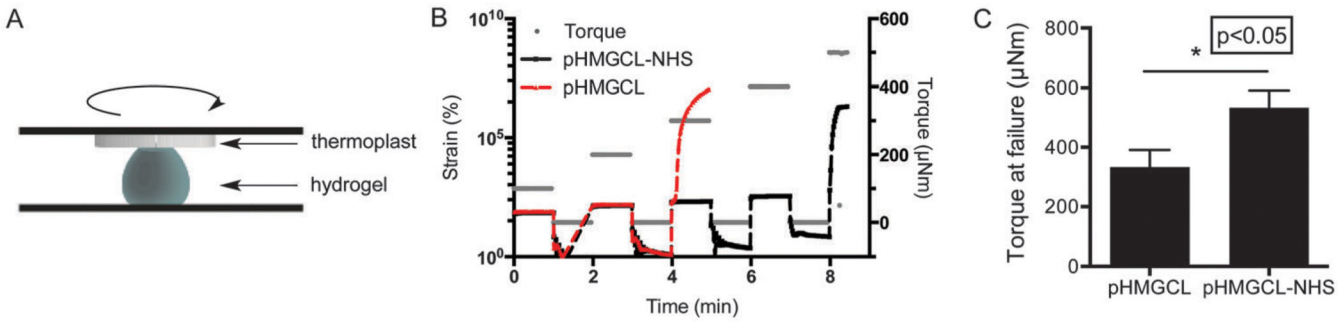

Fig. 6.

Evaluation of hydrogel–thermoplastic integration in creep-recovery tests. (A) Schematic display of the experimental set-up. (B) Representative rheology measurement of creep-recovery between the thermoplastic and the PNC–PEG hydrogel. (C) Torque at failure for PEG–pHMGCL and PEG–pHMGCL–NHS constructs ($n = 3$). $P < 0.05$ was considered as significantly different.

Europe PMC Funders Author Manuscripts

Europe PMC Funders Author Manuscripts

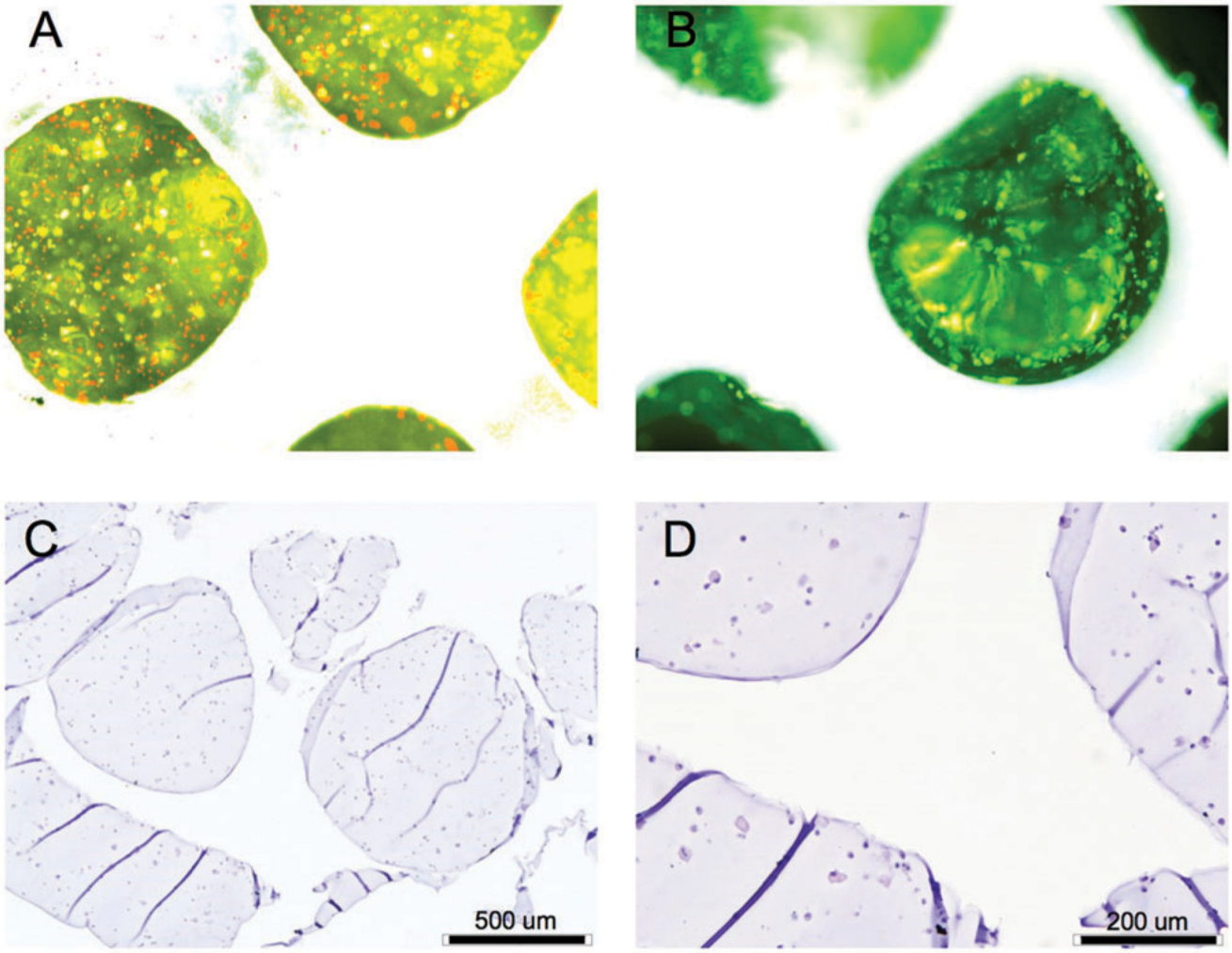

Fig. 7.

Chondrocyte-laden hydrogels reinforced with thermoplastic pHMGCL–NHS network. (A) Representative live (green) and dead (red) staining of reinforced PNC–PEG hydrogels and (B) reinforced PNC–HA hydrogels. The thermoplastic network is shown in white, with the chondrocyte-laden hydrogels in the pores. (C) and (D) Hematoxylin and eosin staining of PNC–PEG hydrogels showing homogeneous cell distribution near the reinforced thermoplastic network.

Europe PMC Funders Author Manuscripts

Table 1

pHMGCL and pHMGCL–NHS characteristics

	Ratio HMG/CL	Ratio NHS/CL	T_m (°C)	T_g (°C)	ΔH_f (J g^{-1})	M_n (kDa)	M_w (kDa)	PDI
pHMGCL	8/92	–	49	−47	65	16.3	22.4	1.4
pHMGCL–NHS	–	8/92	50	−38	53	17.9	23.0	1.3